Journal of Engineering Mathematics 19 (1985) 121–137.

Confined laminar wakes at small and large Reynolds number

R.W. MEI and A. PLOTKIN

Department of Aerospace Engineering, University of Maryland, College Park, Maryland, USA

(Received August 30, 1984 and in final form January 17, 1985)

Summary

The development of the wake flowfield behind a symmetric cascade of finite-thickness flat plates in steady two-dimensional laminar incompressible flow is investigated for a wide range of Reynolds number. A spectral method is used to obtain the solution to a low-Reynolds-number expansion of the Navier-Stokes equations as well as a second approximation to the Oseen equations. Comparisons to the results of the second Oseen approximation are made with previously obtained solutions to the slender-channel equations for large Reynolds number as well as with solutions to the low-Reynolds-number expansion.

1. Introduction

There has been much recent interest in the study of steady two-dimensional laminar incompressible separated flows with closed streamlines. For the most part, fundamental studies consider relatively simple geometries such as occur in wake and channel flows and are concerned with the solution of equations which approximate the Navier-Stokes equations for various Reynolds-number limits. In the limit of small Reynolds number, the Stokes and Oseen equations are often studied. In the large-Reynolds-number limit, the boundary-layer-like slender-channel equations (Williams [1]) as well as the Oseen equations are considered.

For the problem of wake flows at low Reynolds number, Viviand and Berger [2] calculated the wake development behind a blunt-based body with the use of a Fourier-integral solution of the Stokes equations. In order to obtain a qualitative estimate of the effect of the neglected inertia terms on the flowfield, the same technique was used to solve the Oseen equations. The Oseen equations (the Navier-Stokes equations linearized about the free-stream velocity) have also been used to study far-wake flows for a wide range of Reynolds number (see Berger [3]). Plotkin [4] used a Fourier-series spectral method to calculate the Stokes flow behind a cascade of finite-thickness flat plates and obtained results qualitatively similar to those in [2].

Plotkin [3] also used the Fourier-series spectral method to solve the slender-channel equations for the large-Reynolds-number flow behind a cascade of finite-thickness flat plates. The wake flows studied in [2–5] exhibit characteristics similar to those found in the flow through a sudden expansion in a channel, especially at large Reynolds number. Spectral-method solutions to the slender-channel equations for the sudden expansion are given in Kumar and Yajnik [6] and Plotkin [7] and the Oseen-equation solution for this geometry is given by Ramakrishnan and Shankar [8].

In this study, the development of the wake flowfield behind a symmetric cascade of finite-thickness flat plates in steady two-dimensional laminar incompressible flow is investigated for a wide range of Reynolds number. It is the goal of the research to obtain an accurate low-Reynolds-number solution to the Navier-Stokes equations as well as to explore the validity of the second approximation to the Oseen equations for both small and large Reynolds number.

2. Problem formulation and method of solution

Consider the steady two-dimensional laminar incompressible flow past a symmetric cascade of finite-thickness flat plates as shown in Fig. 1. Lengths have been normalized by half the plate separation distance and velocities by the stream velocity; h is the ratio of plate thickness to plate separation. It is intended to calculate the development of the wake from the base of the plate to downstream infinity.

The Navier-Stokes equation in stream-function form is

$$\left(\psi_y \frac{\partial}{\partial x} - \psi_x \frac{\partial}{\partial y}\right) \nabla^2 \psi = R^{-1} \nabla^4 \psi \tag{1}$$

where ψ is the stream function, R is the Reynolds number based on half the plate separation distance and the stream velocity, and ∇^2 and ∇^4 are the Laplace and biharmonic operators. If u and v are the velocity components in the x and y-directions, the stream function is given by $u = \psi_y$ and $v = -\psi_x$.

In general, boundary conditions would be specified far upstream of the base, where the flow is assumed to be fully developed. Here, velocity profiles will be assumed at the base and the wake development will be sought. The solutions obtained will be valid for arbitrary initial profiles. For initial velocity profiles of $u_0(y)$ and $v_0(y)$ and for no disturbance far downstream, the following boundary conditions are obtained:

$$\psi(0, y) = \int_0^y u_0(y)\mathrm{d}y, \tag{2a}$$

$$\psi_x(0, y) = -v_0(y), \tag{2b}$$

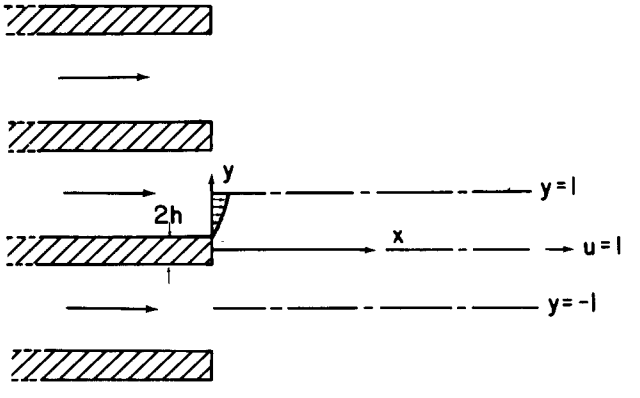

Figure 1. Flow configuration and coordinate system.

$$\psi(\infty, y) = y \quad \text{and} \quad \psi_x(\infty, y) = 0. \tag{2c}$$

The transverse boundaries are symmetry boundaries with

$$\psi(x, \pm 1) = \pm 1, \tag{2d}$$

$$\psi_{yy}(x, \pm 1) = 0. \tag{2e}$$

Since the transverse boundary conditions are periodic, a spectral Fourier-series expansion (as used in Plotkin [4,5]) is taken which identically satisfies equations (2d) and (2e):

$$\psi = y + \sum_{1}^{N} a_n(x) \sin E_n y. \tag{3}$$

The series is truncated after N terms and $E_n = n\pi$. The series is substituted into equation (1) and after the result is multiplied by $\sin E_m y$ and integrated from $y = -1$ to $y = +1$, the following set of coupled nonlinear ordinary differential equations is obtained

$$a_m'''' - Ra_m''' - 2E_m^2 a_m'' + RE_m^2 a_m' + E_m^4 a_m$$
$$- R\sum_n \sum_s \left[C_{mns} a_n' a_s + D_{mns}(a_s a_n''' - a_n' a_s'') \right] = 0. \tag{4}$$

Note that

$$C_{mns} = I_{mns} E_s \left(E_s^2 - E_n^2 \right), \tag{5a}$$

$$D_{mns} = I_{mns} E_s \tag{5b}$$

where

$$I_{mns} = 2\int_0^1 \cos E_s y \sin E_n y \sin E_m y \, \mathrm{d}y \tag{5c}$$

and

$$I_{mns} = \begin{cases} 1/2 & s = n - m,\ m - n, \\ -1/2 & s = n + m, \\ 0 & \text{otherwise.} \end{cases} \tag{5d}$$

The initial conditions, equations (2a) and (2b), are satisfied if

$$a_m(0) = \frac{2}{m\pi} \int_0^1 u_0(y) \cos m\pi y \, \mathrm{d}y \tag{6a}$$

and

$$a_m'(0) = -2\int_0^1 v_0(y) \sin m\pi y \, \mathrm{d}y. \tag{6b}$$

The uniform stream is recovered at infinity so that

$$a_m(\infty) = a'_m(\infty) = 0. \tag{6c}$$

2.1. Low-Reynolds-number expansion

Consider the limit of the foregoing problem for small values of the Reynolds number. Assume an expansion in Reynolds number in the following form:

$$a_m = a_{m_1} + Ra_{m_2} + O(R^2). \tag{7}$$

The function a_{m_1} is the solution of the Stokes-flow ($R = 0$) problem

$$a''''_{m_1} - 2E_m^2 a''_{m_1} + E_m^4 a_{m_1} = 0, \tag{8a}$$

$$a_{m_1}(0) = a_m(0), \quad a'_{m_1}(0) = a'_m(0), \tag{8b}$$

$$a_{m_1}(\infty) = a'_{m_1}(\infty) = 0, \tag{8c}$$

and is given in Plotkin [4] as

$$a_{m_1} = (A_{m_1} + xB_{m_1})\, \mathrm{e}^{-E_m x} \tag{9a}$$

with

$$A_{m_1} = a_m(0), \tag{9b}$$

$$B_{m_1} = m\pi a_m(0) + a'_m(0). \tag{9c}$$

The function a_{m_2} satisfies the following mathematical problem:

$$a''''_{m_2} - 2E_m^2 a''_{m_2} + E_m^4 a_{m_2} = a'''_{m_1} - E_m^2 a'_{m_1} + \sum_n \sum_s \left[C_{mns} a'_{n_1} a_{s_1} + D_{mns}(a_{s_1} a'''_{n_1} - a'_{n_1} a''_{s_1}) \right], \tag{10a}$$

$$a_{m_2}(0) = a'_{m_2}(0) = 0, \tag{10b}$$

$$a_{m_2}(\infty) = a'_{m_2}(\infty) = 0. \tag{10c}$$

The solution for a_{m_2} may be written as

$$a_{m_2}(x) = b_{m_2}(x) + d_{m_2}(x) \tag{11}$$

where b_{m_2} and d_{m_2} are the homogeneous and particular solutions, respectively. b_{m_2} satisfies equation (8a) and is

$$b_{m_2}(x) = (A_{m_2} + B_{m_2} x)\, \mathrm{e}^{-E_m x}. \tag{12}$$

The particular solution satisfies equation (10a) and with the use of equation (9a), the differential equation becomes

$$d''''_{m_2} - 2E_m^2 d''_{m_2} + E_m^4 d_{m_2} = 2B_{m_1}E_m^2 \, e^{-E_m x}$$
$$+ 2\sum_n \sum_s \left\{ I_{mns} E_s \left(E_n^2 B_{n_1} A_{s_1} - E_s E_n B_{s_1} A_{n_1} + E_s B_{n_1} B_{s_1} \right) \right.$$
$$\left. + I_{mns} E_s E_n (E_n - E_s) B_{n_1} B_{s_1} x \right\} e^{-(E_n + E_s)x}. \tag{13}$$

Equation (13) can be solved using the operator method [9] and the solution is

$$d_{m_2}(x) = \frac{B_{m_1}}{4} x^2 \, e^{-E_m x} + \sum_{n=m+1}^{N} \frac{e^{-(2E_n - E_m)x}}{(4E_n(E_n - E_m))^2}$$
$$\times \left\{ \left[E_{n-m} E_n^2 B_{n_1} A_{n-m_1} + E_n^2 B_{n_1} B_{n-m_1} - E_n E_{n-m}^2 A_{n_1} B_{n-m_1} \right] \right.$$
$$\left. + E_n E_m E_{n-m} B_{n_1} B_{n-m_1} x \right\} - \sum_{n=1}^{N-m} \frac{e^{-(2E_n + E_m)x}}{(4E_n(E_n + E_m))^2}$$
$$\times \left\{ \left[E_{n+m} E_n^2 B_{n_1} A_{n+m_1} + E_n^2 B_{n_1} B_{n+m_1} - E_n E_{n+m}^2 B_{n+m_1} A_{n_1} \right] \right.$$
$$\left. - E_n E_m E_{n+m} B_{n_1} B_{n+m_1} x \right\} + \frac{x^2}{8E_m^2} e^{-E_m x} \sum_{n=1}^{m-1} \left\{ \left[E_{m-n} E_n^2 B_{n_1} A_{m-n_1} \right. \right.$$
$$\left. + \frac{E_{m-n}}{E_m} \left(E_{m-n}^2 + E_n^2 \right) B_{n_1} B_{m-n_1} - E_n E_{m-n}^2 B_{m-n_1} A_{n_1} \right]$$
$$\left. + \tfrac{1}{3} E_n E_{m-n} (2E_n - E_m) B_{n_1} B_{m-n_1} x \right\}. \tag{14}$$

The constants A_{m_2} and B_{m_2} in equation (12) can now be obtained by satisfying the initial conditions in equation (10b) with the use of equations (11), (12) and (14). They are

$$A_{m_2} = -d_{m_2}(0), \tag{15a}$$

$$B_{m_2} = -E_m d'_{m_2}(0) - d_{m_2}(0). \tag{15b}$$

2.2. Oseen equations

The Oseen equations (the Navier-Stokes equations linearized about the free-stream velocity) can be used to obtain a qualitative description of the flowfield for a wide range of Reynolds numbers. The approximation can be expected to give its best results when the Reynolds number is small or when the solution is being sought far from a solid body or in a far wake where the disturbance to the uniform stream is small. In the low-velocity recirculation zone of a near-wake region the approximation is expected to be poor.

The Oseen approximation to the Navier-Stokes equation (1) is

$$\left(\nabla^2 - R\frac{\partial}{\partial x}\right)\nabla^2\psi = 0, \tag{16}$$

and the corresponding equivalent of equation (4) is

$$a_m'''' - Ra_m''' - 2E_m^2 a_m'' + RE_m^2 a_m' + E_m^4 a_m = 0. \tag{17}$$

The solution for the cascade (or baffle as it is called in [8]) is discussed in [5] and [8] and is

$$a_m(x) = A_m\, e^{-E_m x} + B_m\, e^{-F_m x} \tag{18a}$$

with

$$F_m = \frac{R}{2}\left[-1 + \left(1 + \frac{4E_m^2}{R^2}\right)^{1/2}\right]. \tag{18b}$$

Satisfaction of the initial conditions of equations (2a) and (2b) yields

$$A_m = \left[F_m a_m(0) + a_m'(0)\right]/(F_m - E_m). \tag{18c}$$

$$B_m = -\left[E_m a_m(0) + a_m'(0)\right]/(F_m - E_m). \tag{18d}$$

3.4. Oseen equations: second approximation

The Oseen equations neglect completely the nonlinear terms in the Navier-Stokes equations (4). To improve the solution, we proceed along the lines of the solution technique for the low-Reynolds-number expansion. An iterative solution is sought of the form

$$a_m(x) = a_{m_1}(x) + a_{m_2}(x) + \ldots \tag{19}$$

where now the function $a_{m_1}(x)$ is the solution to the Oseen equations (17). In this section, therefore,

$$a_{m_1}(x) = A_{m_1}\, e^{-E_m x} + B_{m_1}\, e^{-F_m x}, \tag{20}$$

and A_{m_1} and B_{m_1} are the same as A_m and B_m in equations (18c) and (18d). In the second approximation, $a_{m_1}(x)$ is used to approximate the nonlinear terms in the Navier-Stokes equations (4).

The function a_{m_2} satisfies the following mathematical problem:

$$a_{m_2}'''' - Ra_{m_2}''' - 2E_m^2 a_{m_2}'' + RE_m^2 a_{m_2}' + E_m a_{m_2}$$

$$= R\sum_n \sum_s \left[C_{mns} a_{n_1}' a_{s_1} + D_{mns}\left(a_{s_1} a_{n_1}''' - a_{n_1}' a_{s_1}''\right)\right]. \tag{21a}$$

$$a_{m_2}(0) = a'_{m_2}(0) = 0, \tag{21b}$$

$$a_{m_2}(\infty) = a'_{m_2}(\infty) = 0. \tag{21c}$$

The solution for a_{m_2} may be written as

$$a_{m_2}(x) = b_{m_2}(x) + d_{m_2}(x) \tag{22}$$

where b_{m_2} and d_{m_2} are the homogeneous and particular solutions, respectively. b_{m_2} satisfies equation (17) and is

$$b_{m_2}(x) = A_{m_2} e^{-E_m x} + B_{m_2} e^{-F_m x}. \tag{23}$$

The particular solution satisfies equation (21a). With the use of equation (20), the differential equation (21a) may be written

$$d''''_{m_2} - Rd'''_{m_2} - 2E_m^2 d''_{m_2} + RE_m^2 d'_{m_2} + E_m^4 d_{m_2}$$

$$= R\sum_n \sum_s \left[H_{mns_1} \exp(-\lambda_{ns_1} x) + H_{mns_2} \exp(-\lambda_{ns_2} x) + H_{mns_3} \exp(-\lambda_{ns_3} x) \right] \tag{24a}$$

where

$$H_{mns_1} = I_{mns} E_s (E_n^2 - F_n^2) F_n B_{n_1} A_{s_1},$$

$$H_{mns_2} = -I_{mns} E_s (E_s^2 - F_s^2) E_n B_{n_1} A_{n_1}, \tag{24b}$$

$$H_{mns_3} = I_{mns} E_s (E_n^2 - E_s^2 - F_n^2 + F_s^2) F_n B_{n_1} B_{s_1}$$

and

$$\lambda_{ns_1} = F_n + E_s,\ \lambda_{ns_2} = F_s + E_n,\ \lambda_{ns_3} = F_n + F_s. \tag{24c}$$

With the use of the operator method [9], the solution is obtained as

$$d_{m_2}(x) = R\sum_n \sum_s \sum_{j=1}^{3} H_{mns_j} \exp(-\lambda_{ns_j} x)/Q(\lambda_{ns_j}) \tag{25a}$$

where

$$Q(\lambda) = \lambda^4 + R\lambda^3 - 2E_m^2\lambda^2 - RE_m^2\lambda + E_m^4. \tag{25b}$$

The constants A_{m_2} and B_{m_2} in equation (23) can now be obtained by satisfying the initial conditions in equation (21b). With the use of equations (22), (23) and (25), we have

$$A_{m_2} = \left[-F_m d_{m_2}(0) - d'_{m_2}(0) \right] / (F_m - E_m), \tag{26a}$$

$$B_{m_2} = \left[E_m d_{m_2}(0) + d'_{m_2}(0) \right] / (F_m - E_m). \tag{26b}$$

2.4. Slender-channel equations

In the interest of completeness, the large-Reynolds-number equations used in [5] will also be described. Except in the immediate neighborhood of the base, it is assumed that the streamwise length scale is of order R and the transverse length scale is of order one. If the contracted streamwise coordinate $X = x/R$ is used, the Navier-Stokes equation (1) becomes

$$\psi_{yyyy} = \psi_y \psi_{yyX} - \psi_X \psi_{yyy} + R^{-2}\left[\psi_y \psi_{XXX} - \psi_X \psi_{yXX} - 2\psi_{yyXX}\right] - R^{-4}\psi_{XXXX} \tag{27}$$

and in the large-Reynolds-number limit, the slender-channel equations are

$$\psi_{yyyy} = \psi_y \psi_{yyX} - \psi_X \psi_{yyy}. \tag{28}$$

This is seen to be the Prandtl boundary-layer equation with different scaling and here applies to a fully viscous flow whose pressure gradient is unknown in advance.

The equivalent of equation (4) becomes

$$E_m^2 a_m' + E_m^4 a_m = \sum_n \sum_s C_{mns} a_n' a_s \tag{29}$$

where the prime denotes differentiation with respect to X. Note that the differential equation is now first order in X and it is solved numerically as an initial-value problem with the initial condition of equation (6a).

3. Results and discussion

Strictly speaking, the mathematical problem represented by the ordinary differential equation set (4) with the boundary conditions of equation (6) is the development of the laminar wake downstream of an initial station (the base plane). The flow configuration upstream of this initial station enters the problem through the choice of the base-plane velocity field and it is noted that the solutions presented here are valid for an arbitrary choice of this velocity field.

In what follows, calculations will be presented for an assumed reasonable base-plane velocity field which is compatible with the finite thickness flat plate cascade geometry. The choice of an appropriate initial-velocity field is guided by the analysis of Viviand and Berger [2] for low Reynolds number and by the analysis of Plotkin [5] for large Reynolds number.

The flow upstream of the base is taken to be fully developed and the complete wake flow-field for this confined geometry is fully viscous. The streamwise component of velocity at the base is taken to be the Poiseuille parabolic profile,

$$u_0(y) = \begin{cases} \dfrac{3}{1-h}\left[\dfrac{y-h}{1-h} - \dfrac{1}{2}\left(\dfrac{y-h}{1-h}\right)^2\right] & h \leqslant y \leqslant 1, \\ 0 & 0 \leqslant y \leqslant h \end{cases} \tag{30a}$$

and $u_0(-y) = u_0(y)$. In general, $v_0(y) \neq 0$ due to the upstream influence of the base.

Viviand and Berger [2] suggest a choice such that $v_0(h) = v_0(1) = 0$, $v_0(-y) = -v_0(y)$, and either $v_0 \leqslant 0$ or $v_0 \geqslant 0$ for $h \leqslant y \leqslant 1$. The following parabolic profile is chosen

$$v_0(y) = \begin{cases} V_m\left[1 - \dfrac{4}{(1-h)^2}\left(y - \dfrac{1+h}{2}\right)^2\right] & h \leqslant y \leqslant 1, \\ 0 & 0 \leqslant y \leqslant h. \end{cases} \tag{30b}$$

Substitution of equations (30) into equations (6a) and (6b) gives the following initial values

$$a_m(0) = \frac{6}{\pi^4 m^4 (h-1)^3}[\sin m\pi h + m\pi(1-h)\cos m\pi h], \tag{31a}$$

$$a'_m(0) = \frac{-8V_m}{\pi^3 m^3 (1-h)^2}[2\cos m\pi h - 2\cos m\pi + m\pi(h-1)\sin m\pi h]. \tag{31b}$$

Four different sets of equations have been presented in this study. First, a low-Reynolds-number expansion of the Navier-Stokes equations has been obtained which retains terms linear in R. When the Reynolds number is low, say less than 0.5, the results from this approximation should be quite accurate. The second and third sets of equations are the linear Oseen equations and their second approximation. These equations have the potential to provide a description of the flowfield over a wide range of Reynolds numbers. Fourth, the slender-channel equations are a large-Reynolds-number approximation to the Navier-Stokes equations. The ability of these parabolic equations to adequately represent flowfields which contain recirculation regions is still an open question.

Consider first the low-Reynolds-number regime. In the limit of zero-Reynolds-number, the solutions to the low-Reynolds-number expansion, linear Oseen equations and second Oseen approximation all approach the Stokes-flow result [4]. In this limit, it was found that a recirculation region only appeared behind the base for $V_m > 0$. In this study, $V_m = 0$, 0.2 and $h = 0.5$ are chosen as typical values.

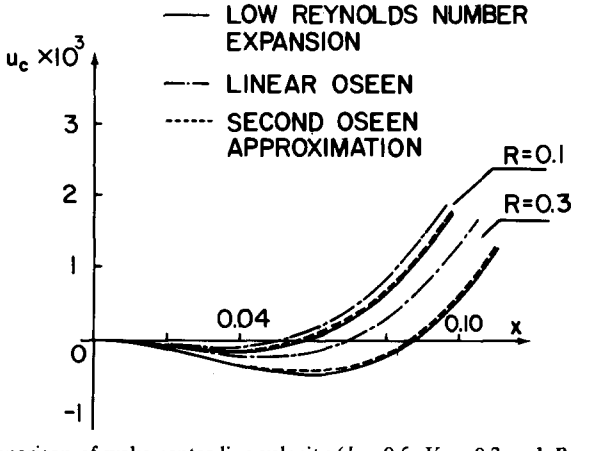

Figure 2. Comparison of wake center-line velocity ($h = 0.5$, $V_m = 0.2$ and $R = 0.1$ and 0.3).

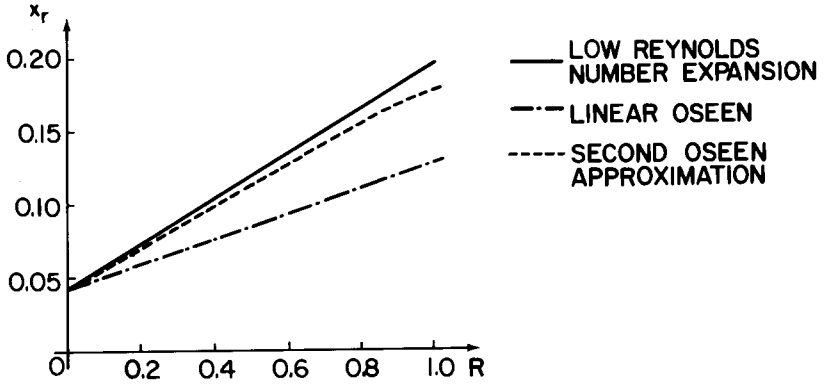

Figure 3. Comparison of length of recirculation region ($h = 0.5$ and $V_m = 0.2$).

Upon examination of the results for the second Oseen approximation as given by equation (25), it was discovered that for $R < 0.8$ and for x within the recirculation region, oscillations in the solution were encountered in the streamwise direction after the series had reached convergence. This behavior was traced to the terms in the summation when $n + s = m$ and the problem was resolved by taking appropriate expansions of the exponential functions for small x and R (see Appendix for the details). The corrected results are used when $R < 0.8$.

Comparisons between the solutions to the low-Reynolds-number-expansion, linear Oseen equations and second Oseen approximation are displayed in Figs. 2–4. In Figs. 2 and 3, the wake center-line velocity u_c and length of the recirculation region x_r are given, respectively, as functions of Reynolds number for $h = 0.5$ and $V_m = 0.2$. Good agreement is noted between the low-Reynolds-numbers expansion and the second Oseen approximation. The ability of the linear Oseen solution to provide a quantitative description of the flow worsens rapidly with Reynolds number increasing from zero. In Fig. 4, the streamline boundary of the recirculation region ($\psi = 0$) is given for $h = 0.5$, $V_m = 0$ and $R = 0.3$. Again the good agreement between the two nonlinear solutions is seen. In Fig. 5 the streamline pattern obtained from the low-Reynolds-number expansion is shown for $h = 0.5$, $V_m = 0$ and $R = 0.3$. The $\psi = 0$ streamline from the low-Reynolds-number expansion is shown as a function of Reynolds number for $h = 0.5$ and $V_m = 0.2$ in Fig. 6.

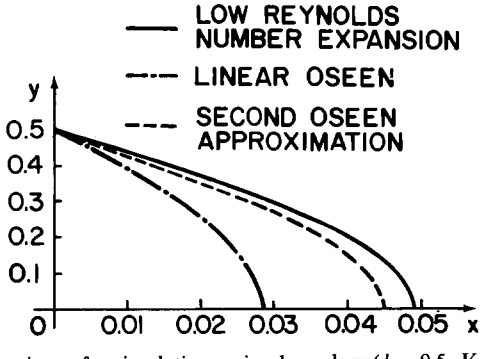

Figure 4. Comparison of recirculation region boundary ($h = 0.5$, $V_m = 0$ and $R = 0.3$).

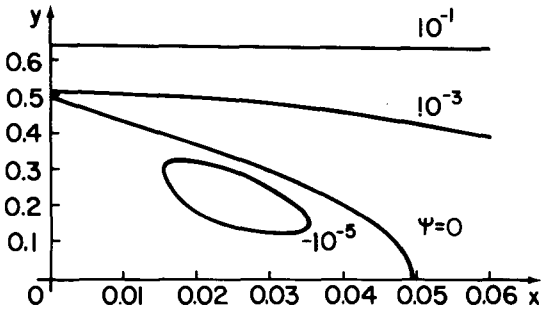

Figure 5. Streamline pattern for low-Reynolds-number expansion ($h = 0.5$, $V_m = 0$ and $R = 0.3$).

Let us now consider a comparison between the solutions of the linear Oseen equations, second Oseen approximation and the slender-channel equations in the large-Reynolds-number limit. In Plotkin [5], it was shown that the number of terms in the Fourier-series solution to the slender-channel equations that could be obtained increased as h approached zero. For $h = 0.2$, an eight-term solution with reasonable convergence properties was found although its accuracy is unconfirmed. In Fig. 7 the wake center-line velocity is compared for $R = 1000$. Close agreement is obtained for x_r between the slender-channel equations and second Oseen approximation but this agreement may be fortuitous. A more meaningful comparison is provided in Fig. 8 which compares the wake center-line velocity for $h = 0$, a cascade of zero-thickness flat plates. This example has no recirculation region so that the slender-channel equations should yield a valid solution. The agreement between the solution to the second Oseen approximation for $R = 10{,}000$ and the slender-channel equations is quite encouraging.

It is seen in the results of Fig. 8 for the second Oseen approximation, in Plotkin [5] for the linear Oseen solution, and in the results of Ramakrishnan and Shankar [8] for the linear Oseen solution for the channel expansion that these equations have a large-Reynolds-number limit which exhibits the proper streamwise scaling. The large-Reynolds-number limit of the second Oseen approximation is explored further in Figs. 9 and 10. In

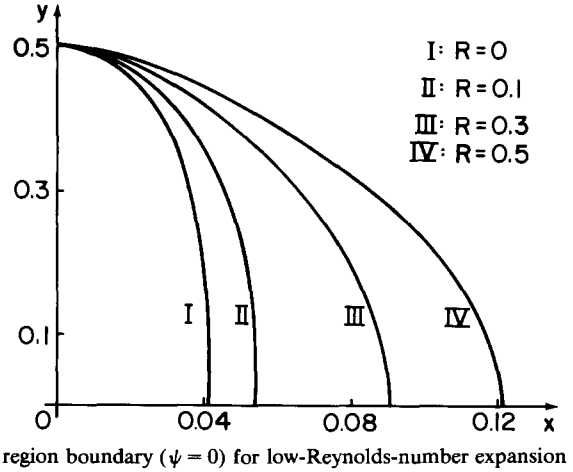

Figure 6. Recirculation region boundary ($\psi = 0$) for low-Reynolds-number expansion ($h = 0.5$ and $V_m = 0.2$).

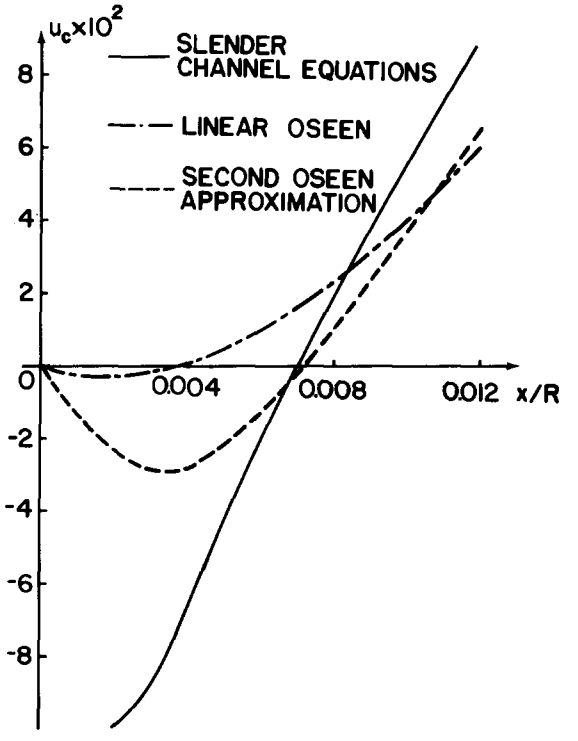

Figure 7. Comparison of large-Reynolds-number wake center-line velocity ($h = 0.2$, $V_m = 0$ and $R = 1000$).

Fig. 9, the $\psi = 0$ streamline for $V_m = 0$ and $h = 0.2$ is plotted versus x/R for $R = 10^n$ and $n = 0$–4. It is noted that in the large-Reynolds-number limit the $\psi = 0$ streamline becomes concave to the flow. In [8] this streamline is concave for all Reynolds numbers. In Fig. 10, the wake centerline velocity for $V_m = 0$ and $h = 0.2$ is plotted versus x/R for $R = 10^n$ and

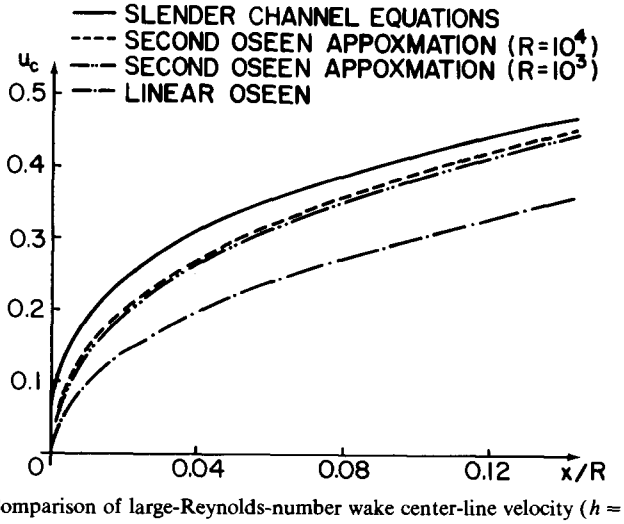

Figure 8. Comparison of large-Reynolds-number wake center-line velocity ($h = 0$, $V_m = 0$).

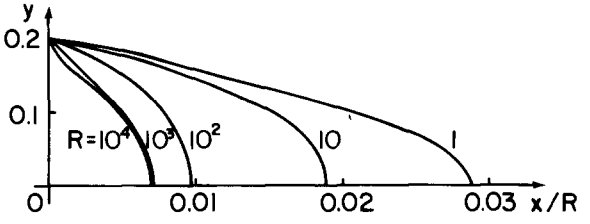

Figure 9. Recirculation region boundary for second Oseen approximation ($h = 0.2$ and $V_m = 0$).

$n = 1$–4 It is seen that the maximum reverse flow velocity reaches a maximum at an intermediate Reynolds number, a result also seen by Viviand and Berger [2]. The large-Reynolds-number limit of the second Oseen approximation is effectively reached when $R = 1000$.

The observation that x scales with R for the second Oseen approximation at large Reynolds number can also be made with an examination of the solution in equation (25). As $R \to \infty$ the following limits hold:

$$F_m = E_m^2 R^{-1},$$

$$\lambda_{ns_1} = O(1), \quad \lambda_{ns_2} = O(1), \quad \lambda_{ns_3} = O(R^{-1}),$$

$$H_{mns_1} = O(R^{-2}), \quad H_{mns_2} = O(R^{-1}), \quad H_{mns_3} = O(R^{-1}),$$

$$Q(\lambda_{ns_1}) = O(R), \quad Q(\lambda_{ns_2}) = O(R), \quad Q(\lambda_{ns_3}) = O(1).$$

The dominant terms in the expansion for $d_{m_2}(x)$ as $R \to \infty$ are therefore of the form $\exp(-aX)$ where a is $O(1)$ and $X = x/R$.

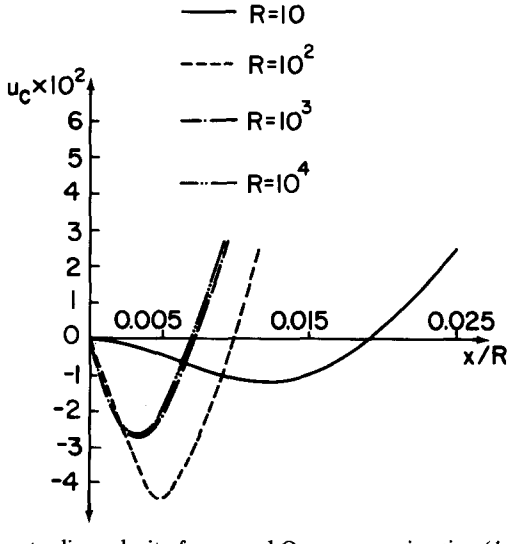

Figure 10. Wake center-line velocity for second Oseen approximation ($h = 0.2$ and $V_m = 0$).

The linear Oseen solution is seen to underpredict the length of the recirculation zone in both the small and large-Reynolds-number limits. The second Oseen approximation is seen to provide results which agree well with the accurate low-Reynolds-number expansion at low Reynolds number and with the slender-channel equations at large Reynolds number. The second Oseen approximation predicts a streamwise length scale of the Reynolds number in the large-Reynolds-number limit (this limit appears to be applicable for Reynolds number greater than approximately 1000). It is speculated that the second Oseen approximation should provide reasonable results for the complete Reynolds-number range.

4. Numerical Navier-Stokes solution

After the above analyses were completed an independent numerical solution of the complete Navier-Stokes equations for the present flow using a semi-implicit single-step finite-difference scheme with second-order accuracy [10] was obtained for low and moderate Reynolds number. The initial (Poiseuille) profiles are properly enforced far upstream of the base so that the correct values of $u_0(y)$ and $v_0(y)$ can be calculated as part of the solution.

A typical calculation for $u_0(y)$ and $v_0(y)$ is shown in Fig. 11a, b and compared to the assumed profiles from equations (30 a, b). The value of V_m is chosen equal to the maximum value of the computed transverse component of the initial profile. It is found that $u_0(y)$ is relatively insensitive to Reynolds number and that the assumed profile is quite reasonable. The transverse component $v_0(y)$ is seen to differ from its assumed parabolic shape. However, when V_m from the numerical solution is used in equation (30b), the second Oseen approximation compares quite well with the Navier-Stokes solution for moderate Reynolds number. This is seen in Fig. 12 where the lengths of the recirculation region from the two calculations are compared.

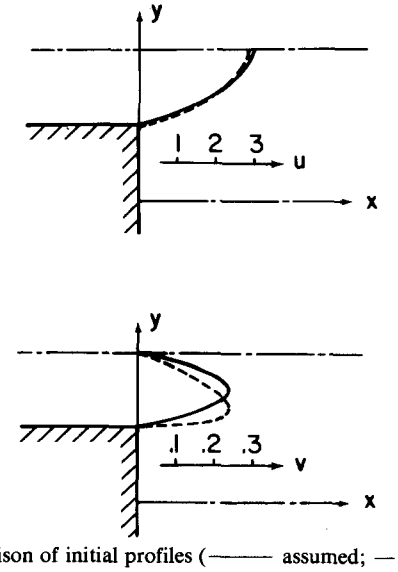

Figure 11. Comparison of initial profiles (——— assumed; — — — Navier-Stokes calculation; $R = 5$, $h = 0.5$) (a) streamwise component and (b) transverse component).

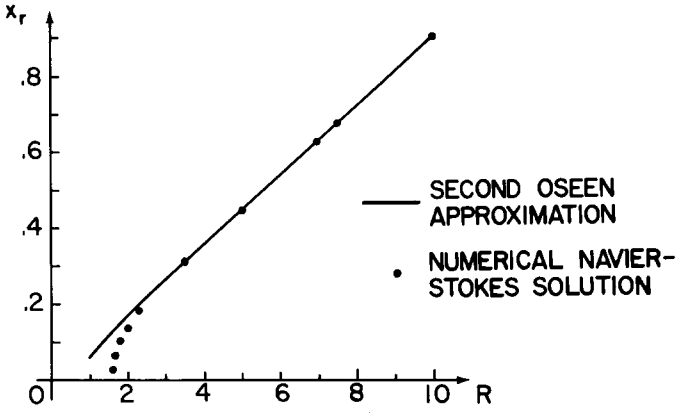

Figure 12. Comparison of length of recirculation region ($h = 0.5$).

The variation of the calculated value of V_m with Reynolds number is shown in Fig. 13. It is seen that V_m is negative and decreases in magnitude with increasing Reynolds number. It appears that V_m is approaching zero as R increases ($V_m = -0.05$ at $R = 50$ and $h = 0.5$) and therefore the choice of $V_m = 0$ for large Reynolds number seems reasonable.

As the Reynolds number approaches zero, both the numerical and analytical results in Fig. 12 suggest the existence of a critical Reynolds number below which no recirculation region occurs. However, the two solutions disagree in this range. This may be due to the choice of the initial profile $v_0(y)$.

Acknowledgment

The authors would like to thank the Computer Science Center of the University of Maryland for supplying them with computer time. This paper, before revision, was originally presented at the AIAA 17th Fluid Dynamics/Plasma Dynamics and Lasers Conference, June 25–27, 1984, Snowmass, Colorado, USA.

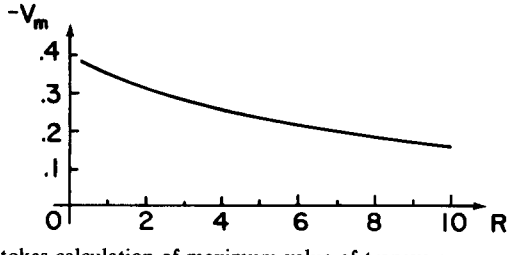

Figure 13. Navier-Stokes calculation of maximum value of transverse component of initial profile.

Appendix

The differential equation and solution for d_{m_2} for the second Oseen approximation are given in equations (24) and (25) as

$$d''''_{m_2} - Rd'''_{m_2} - 2E_m^2 d''_{m_2} + RE_m^2 d'_{m_2} + E_m^4 d_{m_2} = R\sum_n \sum_s \sum_{j=1}^{3} H_{mns_j} \exp(-\lambda_{ns_j} x) \quad \text{(A1a)}$$

where

$$\lambda_{ns_1} = F_n + E_s, \quad \lambda_{ns_2} = F_s + E_n, \quad \lambda_{ns_3} = F_n + F_s, \quad \text{(A1b)}$$

$$d_{m_2}(x) = R\sum_n \sum_s \sum_{j=1} H_{mns_j} \exp(-\lambda_{ns_j} x)/Q(\lambda_{n_s}) \quad \text{(A2a)}$$

where

$$Q(\lambda) = \lambda^4 + R\lambda^3 - 2E_m^2\lambda^2 - RE_m^2\lambda + E_m^4. \quad \text{(A2b)}$$

When $R \to 0$, consider the contribution to the solution (A2a) when $n + s = m$. In this limit,

$$\begin{aligned} F_m &= E_m - R/2 + O(R^2) \\ \lambda_{ns_1} &= E_m - R/2 + O(R^2) \\ \lambda_{ns_2} &= E_m - R/2 + O(R^2) \\ \lambda_{ns_3} &= E_m - R + O(R^2) \end{aligned} \quad \text{(A3)}$$

and, after substitution into equation (A2b), it is seen that $Q(\lambda) = O(R^4)$. This leads to streamwise oscillations in the solution (A2a) within the recirculation region.

The root of this problem lies in the exponential terms in the differential equation (A1a). It can be corrected by applying a consistent small R approximation to these terms. Define

$$\begin{aligned} \beta_1 &= E_n - F_n, \quad \beta_2 = E_s - F_s, \\ \beta_3 &= E_n - F_n + E_s - F_s \end{aligned} \quad \text{(A4)}$$

and note $\beta_i = O(R)$. When $n + s = m$,

$$\exp(-\lambda_{ns_1} x) = \exp(-E_m x)\exp(\beta_1 x) = \exp(-E_m x)\left[1 + \beta_1 x + O(\beta_1 x)^2\right]. \quad \text{(A5)}$$

Similarly,

$$\exp(-\lambda_{ns_2} x) = \exp(-E_m x)\left[1 + \beta_2 x + O(\beta_2 x)^2\right],$$

$$\exp(-\lambda_{ns_3} x) = \exp(-E_m x)\left[1 + \beta_3 x + O(\beta_3 x)^2\right].$$

Equation (A5) is substituted into equation (A1) for $n + s = m$ and, if only the linear terms in the expansion are kept, use of the operator method leads to the contribution to d_{m_2} of

$$\bar{d}_{m_2}(x) = \frac{-x \exp(-E_m x)}{2E_m^2} \sum_{\substack{n \\ n+s=m}} \sum_{s} \sum_{j=1}^{3} H_{mns_j}\left[1 + \alpha_1\beta_j + \tfrac{1}{2}\beta_j x\right] \tag{A6a}$$

where

$$\alpha_1 = (4E_m + 3R)/2RE_m. \tag{A6b}$$

For $R < 0.8$, the solution for d_{m_2} that is used is

$$d_{m_2}(x) = R \sum_{\substack{n \\ n+s\neq m}} \sum_{s} \sum_{j=1}^{3} H_{mns_j} \exp\left(-\lambda_{ns_j} x\right)/Q\left(\lambda_{ns_j}\right) + \bar{d}_{m_2}(x). \tag{A7}$$

Further analysis shows that neglect of the quadratic terms in the expansion of the exponentials in equation (A5) leads to errors of order

$$O\left[\left(R^4x^2 + R^4x^3\right) \exp(-E_m x)\right]$$

so that use of the linear terms alone is justified for the complete range of x.

References

[1] J.C. Williams, Viscous compressible and incompressible flow in slender channels, *AIAA Journal* 1 (1963) 186–195.

[2] H. Viviand and S.A. Berger, The base-flow and near-wake problem at very low Reynolds numbers; Part I, The Stokes approximation; Part II, The Oseen approximation, *Journal of Fluid Mechanics* 23 (1965) 417–458.

[3] S.A. Berger, *Laminar Wakes,* American Elsevier Publishing Co, Inc., New York (1971).

[4] A. Plotkin, Development of confined Stokes flow wakes, *AIAA Journal* 20 (1985) 349–353.

[5] A. Plotkin, Development of confined laminar wakes at large Reynolds numbers, *AIAA Journal* 20 (1982) 211–217.

[6] A. Kumar and K.S. Yajnik, Internal separated flows at large Reynolds number, *Journal of Fluid Mechanics* 97 (1980) 27–51.

[7] A. Plotkin, Spectral method solutions for some laminar channel flows with separation, *AIAA Journal* 20 (1982) 1713–1719.

[8] S.V. Ramakrishnan and P.N. Shankar, The Oseen model for internal separated flows, *Journal of Engineering Mathematics* 16 (1982) 325–347.

[9] L.M. Kells, *Elementary Differential Equations,* McGraw-Hill, New York (1954) 74–77 and 86–89.

[10] R.W. Mei and A. Plotkin, A semi-implicit single-step scheme of a time-dependent technique for solving the steady Navier-Stokes equations, submitted for publication.